Semi-Automatic Detection of Calcified Plaque in Coronary CT Angiograms with 320-MSCT

Yuki Yoshida, Kaori Fujisaku,
Kei Sasaki, Tetsuya Yuasa

Graduate School of Science and Engineering
Yamagata University
Yonezawa, Japan
yyj.yks@gmail.com

Koki Shibuya

Division of Radiology
Nihonkai General Hospital
Sakata, Japan
radt009@nihonkai-hos.jp

Abstract— **Coronary CT angiography (Coronary Computed Tomography Angiography) by MSCT (Multi-Slice Computed Tomography) offers not only a diagnostic capability matching that of CAG (Coronary Angiography) that is the gold standard of the cardiovascular diagnosis, but also a much less invasive examination. However, if calcified plaque adheres to a vessel wall, high brightness shading due to calcium in the calcified plaque, called the blooming artefacts, causes to make it difficult to diagnose the region around the plaque. In this study, we propose a method to semi-automatically detect and remove calcified plaques, which hinder diagnosing a stenosed coronary artery, from a CCTA image. In addition, an analyzing method to accurately and objectively measure angiostenosis rate is provided.**

Keywords- ***MSCT (multi-slice computed tomography), CTA (computed tomographic angiography), coronary artery, calcified plaque***

I. INTRODUCTION

The number of patients suffering from ischemic heart disease such as angina pectoris and myocardial infarction, which are caused by hardening of coronary arteries, is increasing every year, and ischemic heart disease holds the second place in cause of death in Japan, following cancer. While an invasive catheterization study, *i.e.*, coronary angiography (CAG), has been so far performed as the gold standard of cardiovascular diagnosis, CAG involves risks of complications such as bleeding, hemorrhage, vasospasm, perforation, vascular injury, and hematoma at a probability of about 1.0 %, and especially the probability of fatal complication amounts to 0.05 to 0.2 %.

Recently, multi-slice CT (MSCT) with higher spatial and temporal resolution has become available widely. With the introduction of MSCT, coronary CT angiography (CCTA) is expected as an attractive diagnostic method for cardiovascular diseases [1], because the risk of serious side effects caused by using iodine contrast agent is very low, and CCTA with MSCT offers 3-D information about coronary arteries with much less motion artifacts, leading to more precise diagnosis.

However, in the case that a calcified plaque adheres to a vascular wall, it generates brightness shading called blooming artefacts around the plaque. Then, CCTA tends to overestimate the angiostenosis rate [2]. In order to circumvent the difficulty, calcified plaques are carefully removed using an interactive image processing software by radiographers before the diagnosis. However, the procedure takes about an hour per patient because many image processing techniques are sequentially applied while manually adjusting some parameters in order to precisely remove the plaques, and in addition the procedure cannot always offer objective results because it is dependent on the performance of the software and the skill of radiographer.

In this study, in order to provide a reliable and objective cardiovascular diagnosis with less efforts, we developed a preliminary CAD (computer assisted diagnosis) system to semi-automatically detect the calcified plaques and to objectively analyze the angiostenosis rate.

II. MATERIALS AND METHOD

A. Coronary CT Angiograms

We assessed 7 patients who have stenosis by calcified plaques in coronary artery. CCTA inspection on them were performed using 320-detector row MSCT "Aquilion ONE" manufactured by Toshiba Medical Inc. (voltage: 120 kVp, current: 520 to 580 mA, scan time / rotation: 0.5 s, image size: $512 \times 512 \times 640$, voxel size: $0.35 \times 0.35 \times 0.5$ mm^3). The ethics committees of both the Nihonkai General Hospital and Yamagata University approved this study, and all subjects gave written informed consent to participate.

B. Algorithm

The procedure is broadly divided by three modules which are sequentially performed: (1) extraction of coronary arteries, (2) detection of calcified plaques, and (3) measurement of constriction rate. A simple thresholding cannot precisely

978-0-9928-6265-7/16/$31.00 ©2016 IEEE

extract both coronary artery (CA) and calcified plaque (CP) because their CT values are similar to those of bone regions. Therefore, throughout the procedure, a recognition technique of 3-D object plays an important role, since we can regard CA and CP as a line-like and a blob-like objects, respectively.

Eigenvalue analysis of Hessian is very effective to 3-D object recognition [3,4]. Letting $I(\boldsymbol{x})$ be a brightness at coordinate $\boldsymbol{x} = (x, y, z)^t$, Hessian $H(\boldsymbol{x})$ at $\boldsymbol{x}$ is given as

$$H(\boldsymbol{x}) = \begin{pmatrix} I_{xx} & I_{xy} & I_{xz} \\ I_{yx} & I_{yy} & I_{yz} \\ I_{zx} & I_{zy} & I_{zz} \end{pmatrix}, \quad (1)$$

where, for example, I_{xx} is a second order differentiation value with respect to x, and other elements are defined in the same way. Letting λ_1, λ_2, and λ_3 ($|\lambda_1| \geq |\lambda_2| \geq |\lambda_3|$) be eigenvalues of $H(\boldsymbol{x})$, the magnitude correlation among the eigenvalues is related to a local structure of $I(\boldsymbol{x})$ around $\boldsymbol{x}$ as shown in TABLE 1 [3,4]. Based on the concept, we below describe each module in detail.

TABLE 1 Possible patterns in 3D, depending on the value of the eigenvalues λ_k (H = high, L = low) [4].

$\lvert\lambda_1\rvert$	$\lvert\lambda_2\rvert$	$\lvert\lambda_3\rvert$	Structural Pattern
H	L	L	Plate-like
H	H	L	Line-like
H	H	H	Blob-like

1) Extraction of Coronary Arteries: Although we will extract CAs using a filter enhancing the line-like structure based on the eigenvalues of Hessian, we in advance remove unnecessary regions as preprocessing. In CCTA, CT values in CAs broadly range from 100 to 2000 HU. First, we remove the regions below 0 HU using a simple thresholding, because they may include pulmorary arteries or veins which are enhanced by the line-enhancing filter. Next, we remove the regions having higher CT values such as bone, which may be detected falsely as CAs. However, the CT values of CAs are similar to those of bone. Thus, the higher CT-value regions are removed using the 3-D region grwoing method, in which the seed point and the permissible range of CT value are set and adjusted manually.

Then, the following line-enhancing filter $V(\boldsymbol{x})$, which gives a relatively higher value in the case that λ_1 and λ_2 are high and λ_3 is low, *i.e.*, the object is line-like, and a lower value otherwise [4], is applied to the preprocessed CCTA image:

$$V(\boldsymbol{x}) = \left(1 - \exp(-\frac{R_1^2}{\alpha})\right)\exp(-\frac{R_2^2}{\beta})\left(1 - \exp(-\frac{T^2}{\gamma})\right), \quad (2)$$

where

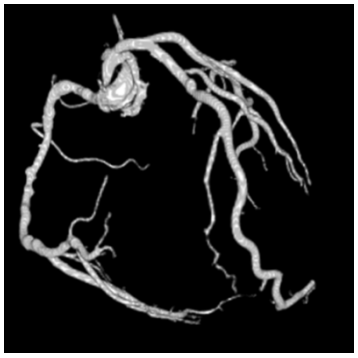

Fig. 1 Extracted coronary artery (volume rendering representation)

$$R_1^2 = \left(\lambda_2 / \lambda_3\right)^2, \quad R_2^2 = \lambda_1^2 / |\lambda_2\lambda_3|, \quad T^2 = \sum_{k=1}^{3} \lambda_k^2, \quad (3)$$

and α, β, and γ are constants. From TABLE 1, only when a local structure is line-like, the first and second terms of $V(\boldsymbol{x})$ are moderate, and otherwise, they are minuscule. The third term suppresses the influence due to background noise. Therefore, 3-D image $V(\boldsymbol{x})$ generated from $I(\boldsymbol{x})$ takes higher values at the positions where the local structure around $\boldsymbol{x}$ is line-like. In this research, the elements of Hessian were obtained by convolving $I(\boldsymbol{x})$ with a second derivative of Gaussian. And, $\alpha = \beta = 0.5$, and $\gamma = 2.0 \times \max T^2$, where max T^2 is the maximum of T^2 in the CCTA image.

Finally, we extract CAs by applying the 3-D region growing method to the line-enhanced image $V(\boldsymbol{x})$, in which the seed point and the permissible range of pixel value are set and adjusted manually. An example of the result is shown in Fig. 1.

2) Detection of Calcified Plaque: CPs can be relatively easily found by applying a simple thresholding to the result in the previous processing, because they are adheres to the CAs and they have CT values higher than those in the CAs. However, it is very difficult to precisely detect the contour of CP. Figure 2 shows the zoomed region including CA and CP in the axial image of the original CCTA. From Fig. 2, the boundary between CA and CP regions is not clear. So, in order to increase the precision of detecting boundaries, the CP regions are enhanced with the following two-step processing based on their blob-like features

First, we enhance the CP as a blob-like object using the blob-enhancing filter which was devised based on the fact listed in TABLE 1. The following blob-enhancing filter $W(\boldsymbol{x})$, which gives a lower value in the case that the object is plane- or line-like, and a relatively higher value in the case the object is blob-like, is applied to the coronary-artery-extracted image:

$$W(\boldsymbol{x}) = \exp(-\frac{R_1^2}{\alpha})\exp(-\frac{R_3^2}{\delta})\left(1 - \exp(-\frac{T^2}{\gamma})\right), \quad (4)$$

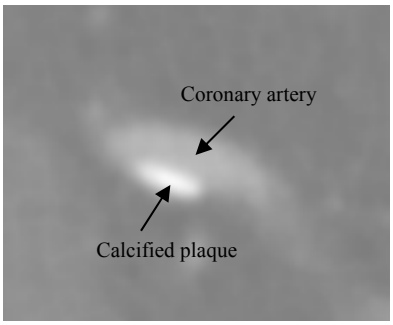

Fig. 2 Zoomed image of region including coronary artery and calcified plaque.

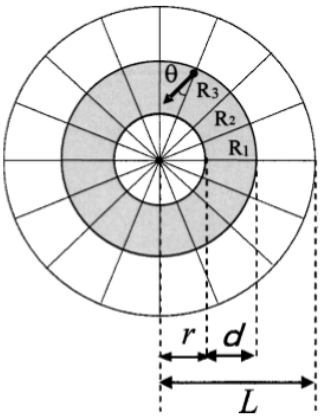

Fig. 3 Support region of the convergence index filter. Actual support is three dimensional.

where

$$R_1^2 = \left(\lambda_2 / \lambda_3\right)^2, \quad R_3^2 = \left(\lambda_1 / \lambda_2\right)^2, \quad T^2 = \sum_{k=1}^{3} \lambda_k^2, \quad (5)$$

and α, γ, and δ are constants. From TABLE 1, only when a local structure around $\boldsymbol{x}$ is blob-like, the first and second terms of $W(\boldsymbol{x})$ are moderate, and otherwise, they are minuscule.

Next, in order to further enhance the boundary between the CP and CA regions, we pay attention to the fact that the profile of a CP region of the resultant image in the previous processing is unimodal, i.e., the gradient vectors in the CP region are oriented to its centroid. Then, we further enhance the CP regions using the 3-D convergence index filter for vector fields [5,6]. Letting R_i ($0 \le i \le N-1$) be a ray in a 3-D Euclidean space originating from a point of interest $\boldsymbol{x}$, the output of the filter is as follows:

$$C(\boldsymbol{x}) = \max_{0 \le r \le L-d} \frac{1}{N} \sum_{i=0}^{N-1} c_i, \quad (6)$$

where

$$c_i = \frac{1}{d} \sum_{j=d+1}^{R} \cos\theta_{ij}. \quad (7)$$

Fig. 4 Detected calcified plaque

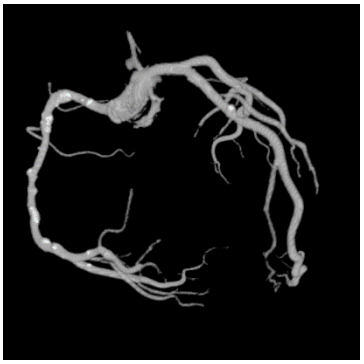

Fig. 5 Fusion image of coronary arteries and calcified plaques. Coronary arteries are represented in volume rendering. Calcified plaques are represented in white.

Here, r and R ($R = r + d$) are inner and outer radii of the support, respectively; d is a width of the support; L is a predefined radius; c_i is the convergence index on the ray R_i, and θ_{ij} is an angle between the ray R_i and the gradient vector on the jth pixel on the ray R_i (Fig. 3).

Finally, the CP regions are detected by thresholding the resultant image with a threshold of $1/\pi$. Figure 4 shows the detected result of a CP region, which is shown in Fig. 2. Figure 5 shows a fusion image of CA and CP regions.

3) Measurement of Angiostenosis Rate: In order to objectively measure an angiostenosis rate, the plane, P, which contains a point of interest in a CP region and is vertical to a blood vessel in the vicinity of the CP is needed. The angiostenosis rate is defined as the ratio of an cross sectional area of CP region to that of CA region in plane P.

First, a point of interest, $\boldsymbol{y}$, in a CP region is selected manually. Next, we regard a segmental blood vessel around $\boldsymbol{y}$ as a cylinder, and define a vector $\boldsymbol{v}$ vertical to plane P as an axis of the cylinder. For obtaining $\boldsymbol{v}$, we first calculate eigenvalues from Hessians $H(\boldsymbol{y}_k)$ at point, $\boldsymbol{y}_k$, in a region in a segmental blood vessel around $\boldsymbol{y}$, R_y, and then obtain an eigenvector coresponding to the smallest absolute eigenvalue $\boldsymbol{e}_k$. We define the vector $\boldsymbol{v}$ as the average vector of all vectors $\boldsymbol{e}_k$ such that $\boldsymbol{y}_k \in R_y$.

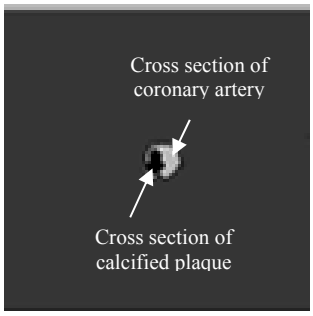

Fig. 6 Measurement of angiostenosis rate

Next, we rotate the segmental blood vessel R_y using a rigid body conversion so that the orientation of cylindrical axis corresponds with that of the z-axis. Figure 6 shows the cross section of stenosed CA with a CP in the plane vertical to the blood vessel.

Finally, we calculate the ratio of a cross sectional area of CP to that of CA, which is an angiostenosis rate.

III. Experiments and Results

A. Physical Phantom

We evaluated the accuracy of the proposed method using a hand-made physical phantom. First, we smashed an oyster shell into powder, and then mixed the powder with glue for wood and pasted the mixed glue, simulating a calcified plaque, to an inner wall of a drinking straw, simulating a blood vessel, after shaping the glue to a sphere, where the diameters of cross section of straw and of a glue sphere were about 5.0 mm and 2.0 mm, respectively. Then, we filled the straw with an iodine solution simulating a contrast agent, and put it in 30-cm-in-diameter acrylic cylinder filled with water. We obtained a CT image of the phantom using Aquilion ONE. We applied the proposed algorithm to the image, and obtained 3.98 mm^3 as the volume of fake plaque, and 14.7 % as the angiostenosis rate, while the theoretical values were 4.19 mm^3 (= 4 π / 3 mm^3) and 16 % (= 1.0^2 / $2.5^2 \times$ 100), respectively. Therefore, the precision are 95.0 % (= 3.98 / 4.19 × 100) for the volume and 92.0 % (= 14.7 / 16 × 100) for the angiostenosis rate.

B. Clinical Images

For the clinical images acquired from 7 patients, we compared the number of CPs detected by a skillful radiographer using a commercial interactive software with that detected using the proposed method. In this study, we subjectively evaluated the correspondence from their 3-D position regardless of their shape and volume. The results are listed in TABLE 2. Although this study was subjective, the precision was 94.4 %. Some CPs were missed in the case that the CT-value difference between the CP and CA is less than 300, and in the case that the regions including lots of small fractional CPs exist. For the former and latter cases, the selections of thresholding level to detect CAs and of range in the convergence index filter seemed to be inadequate, respectively. We should investigate how to select the adequate parameters automatically.

TABLE 2 Correspondence between manual detection by a skillful radiographer and semi-automatic detection by the proposed method.

	Patient *1*	Patient *2*	Patient *3*	Patient *4*	Patient *5*	Patient *6*	Patient *7*
Manual Detection	3	4	5	8	4	30	17
SemiAutomatic Detection	3	4	5	7	3	29	16

IV. Conclusion

In this research, we proposed a novel practical image processing technique to detect calcified plaques hampering to diagnose vessel lumen from CCTA image using MSCT. The efficacy of the proposed method was demonstrated using the CT image of a hand-made physical phantom. In addition, the extremely high correspondence between semi-automatic detection by the method and manual detection by a skillful radiographer was shown using clinical data. However, the evaluation was based on the position of the CP detected, and its shape and volume were not verified quantitatively. Futuristic work will be to demonstrate precision and quantifiablity of the proposed method by morphologically and quantitatively comparing the result by the method with that measured by IVUS (intravascular ultrasound) or cardiovascular OCT (optical coherence tomography) with much higher resolution.

The proposed algorithm had many hyper-parameters, for example, α, β, γ, and δ in the filters to detect CAs and CPs, r, d, L, and N in the convergence index filter, and some thresholding levels. In the experiment, we set them by trial and error. The problem should be solved in order to aim at fully automatic processing.

In the present clinical scene, the angiostenosis rate is calculated from 2-D coronary angiogram. On the other hand, we proposed a novel method to 3-dimensionally measure the angiostenosis. The efficacy should be investigated clinically.

References

[1] S. Leschka, H. Alkadhi, A. Plass, L. Desbiolles, J. Grünenfelder, B. Marincek, S. Wildermuth, "Accuray of MSCT coronary angiography with 64-slice technology: first experience," European Heart Journal, Vol. 26, pp. 1482-1487, 2005.

[2] A. Ikai, Y. Lee, D. Tsai, I. Yamamoto, K. Matsumoto, M. Kimura, "Improvement of Determination Technique for Extractiong Centerline in Coronary Artery with Calcification on CTA," Nihon Hoshasen Gijutu Gakkai Zasshi, Vol.65, No.9, pp.1313-1323, 2009.

[3] Y. Sato, S. Nakajima, N. Shiraga, H. Atsumi, S.Yoshida, T.Koller, G. Gerig and R. Kikins, : 3D multi-scale line filter for segmentation and visualization of curvilinear structures in medical images, Medical Image Analysis, vol. 2, no. 2, pp. 143-168, 1998.

[4] A. F. Frangi, et al.: Multiscale vessel enhancement filtering, MICCAI'98, Lecture Notes in Computer Science, Vol. 1496, pp.130-137, 1998.

[5] H. Kobatake, S. Hashimoto, "Convex Index Filter for Vector Fields," IEEE Trans. Image Processing, Vol. 8, No. 8, pp. 1029-1028, 1999.

[6] J. J. Suarez-Cuenca, P. G. Tahoces, M. Souto, M. J. Lado, M. R. Jardin, J. Remy, J. J. Vidal, "Application of the iris filter for automatic detection of pulmonary nodules on computed tomography images," Computers in Biology and Medicine, Vol. 39, pp. 921-933, 2009.